Int. J. Morphol.,
43(2):351-359, 2025.

Bioscaffold Sponge with *Hippophae rhamnoides* L Accelerates Burn Wound Repair: *in vitro* and *in vivo* Studies

La Esponja de Bioandamio con *Hippophae rhamnoides* L Acelera la Reparación de Heridas por Quemaduras: Estudios *in vitro* e *in vivo*

Ming Xu[1]& Xingyu Zhu[2]

XU, M. & ZHU, X. Bioscaffold sponge with *Hippophae rhamnoides* L accelerates burn wound repair: *In vitro* and *in vivo* studies. *Int. J. Morphol., 43(2)*:351-359, 2025.

SUMMARY: Several wound-dressing materials have functional and structural flaws that limit them from facilitating wound healing. Accelerating blood coagulation, preventing bacterial infection, and starting the regeneration process in full-thickness wounds are all possible outcomes of the design of multifunctional wound dressings. Herein, *Hippophae rhamnoides* L (HRL), a traditional Chinese herb, was combined with substituted hydroxyapatite (SHA)/alginate (ALG)/carboxymethyl cellulose (CMC) (HSAC) via freeze-drying, electrostatic attraction, and ecofriendly crosslinking techniques to make multifunctional bioscaffold sponges. HSAC samples cell proliferation was highly enhanced compared to control for different cell culture times. While *in vivo* study was carried out using an excisional wound model, *in vitro* investigations were carried out utilizing toxicity and wound healing assays. Histology was performed on tissues extracted from the wound region. We observed the wound healing process throughout the one, three, and fourteen days. The HRL-containing bioscaffold sponge formulation performed better than the control group when wound construction was evaluated. Histological analysis showed that the HRL formulation induced skin regenerative activity. The wound healing experiment utilizing HUVEC cells revealed significant cell proliferation when HRL-bioscaffold sponges were used. Finally, both ex vivo and *in vivo*, our test material HSAC bioscaffold sponges significantly accelerated wound healing.

KEY WORDS: Bioscaffold; Antibacterial activity; Burn wound; Herbal; Wound healing.

INTRODUCTION

According to clinical data, a growing proportion of burns are not healing, which has had a significant financial impact on the world's healthcare system (Saavedra *et al*., 2021; Jafari *et al*., 2021). Various techniques are now being used to address the clinical aspects of burns. Biological dressings are a special kind of material for prevention and cure that follow the wet healing principle. Due to their many advantages, such as being robust biomaterials and possessing properties that are neither irritating nor dangerous, biopolymers with a variety of biological and physicochemical characteristics have been extensively investigated as wound dressings (Kamoun *et al*., 2017).

Particularly, alginate (ALG) is a polymer derived primarily from brownish algal biomass.

Recent years have seen a significant increase in the usage of ALG-based composites in therapeutic settings, including tissue engineering and drug delivery, due to their cytocompatibility, degradability, ease of gel development, and low price (Sahoo & Biswal, 2021; Raus *et al*., 2021). Biomaterials made from pure ALG prevent an inflammatory response in tissue engineering while fostering osteoblastic growth in bone-forming cells (Hegde *et al*., 2022). However, it still has several limitations, such as delayed hemostasis, inability to prevent microbial invasion, difficulty in reducing scar formation and promoting vasculature, and so forth. Carboxymethyl cellulose (CMC) is a water-soluble cellulose derivative that contains a carboxymethyl functional group. It has gained significant attention due to its impressive properties such as thrombolytic, bactericidal, and cytocompatibility (Widiyanti & Priskawati, 2023). Furthermore, the ALG/CMC biocomposites has insufficient biological properties to activate cells, making it difficult to divert skin defects into a recovery process (Chang *et al*., 2022).

[1] Pharmaceutical Department, the First Hospital of Tsinghua University, Beijing, China.
[2] University of Technology and Science Beijing School of Mathematics and Physics U202242316, Haidian District, Beijing, China.

Received: 2024-09-23 Accepted: 2024-12-05

Biologically and agriculturally significant, hydroxyapatite (HA) is a naturally occurring bioceramic biomaterial generated from calcium phosphate (CaP) as a mineral source. HA biological and physical characteristics can be drastically altered by structural changes (Wang & Shi, 2022). As a result, substituting the material with copper and zinc ions gives it bactericidal qualities that reduce inflammation and encourage new bone development, which is critical for operations. Previous study has documented the modification of hydroxyapatite through the incorporation of copper or zinc ions (Yu *et al*., 2022; Kumar & Mohanty, 2023). Furthermore, the exact location of substitution minerals ions in the hydroxyapatite structure is yet unknown. It would be possible to use HA as a scaffold to create a stable biocomposite structure, which would let the biocomposite active ingredients and the burn tissue's effect work together to speed up the healing process.

Traditional Chinese medicine originating from plants, mammals, and invertebrates had productive ecosystems in facilitating the healing of wounds in Chinese Civilization. Specifically, Chinese medication called *Hippophae rhamnoides* L (HRL) is frequently used in therapeutic settings. HRL leaf, fruits, and nuts have all been shown to have wound healing properties (Chen *et al*., 2023; Ma *et al*., 2023). According to a recent review conducted by Pundir *et al.* (2021) HRL leaf extract considerably improved wound closure in rat full-thickness wound treatments. It was also shown that HLR leaf extract may raise the levels of antioxidants and vitamin C in wounds, accelerate collagen production, and vascularization by upregulating the expression of vascular endothelial growth factor in newly-regenerated tissue. Moreover, it is uncertain which active elements are important in the aforesaid impacts (Zhang *et al*., 2021).

Sponge dressings have recently been developed for wound repair because of their outstanding physical modulus, which protects skin wounds without causing damage, large porous structure, which helps with gas permeability and water vapor volatilization, high specific surface area, which helps with wound exudate uptake and inhibition of platelet aggregation, and large number of pores that help with wound exudate uptake. Sponge structure offers excellent potential for speeding the healing process because of the outstanding characteristics listed above.

Based on the findings above, it is reasonable to propose that HLR/SHA/ALG/CMC (HSAC) bioscaffold sponges could provide favorable physiochemical properties stimulation to advance blood coagulation, significantly affect bacteremia, attenuate the restorative extracellular matrix, and thus stimulate wound healing, which has not previously been published. In order to test the aforementioned concept, multipurpose bioscaffold sponges were produced in this research by incorporating HLR into SHA/ALG/CMC via freeze drying method. The bactericidal characteristics and hemocompatiblity of the bioscaffold sponges were investigated. Furthermore, the cell counting kit-8 (CCK-8) assays were used to evaluate the cytocompatibility of the prepared samples. Ultimately, a rat back burn model was constructed to evaluate the efficacy of HSAC bioscaffold sponge as burn dressings. Our findings suggest that multipurpose HSAC bioscaffold sponges have considerable potential value for burn wound healing.

MATERIAL AND METHOD

Preparation of hydroxyapatite (SHA): The microwave-assisted approach was used to synthesize SHA with Cu and Zn in the chemical molar ratio $Ca_{9.5}Mg_{0.25}Sr_{0.25}(PO_4)_6(OH)_2$. Calcium nitrate tetrahydrate, copper nitrate, zinc nitrate, and di-ammonium hydrogen phosphate were chosen as the initial calcium, copper, zinc, and phosphate precursors, respectively. Deionized water was used to create a crystal-clear aqueous solution by dissolving the specified quantities of Ca, Cu, and Zn minerals. In addition, the specified quantities of di-Ammonium hydrogen phosphate were dissolved in deionized water to produce a P precursor solution. To create a solution with a (Ca + Cu + Zn)/(P) ratio of 1.67, this solution was gradually added to the mineral's precursor solution. After that, NaOH was continuously poured into the mixture while it was being stirred to raise the p^H to 10. The solution was put in a microwave, and microwave irradiation at 850 W was delivered for 10 min under atmospheric conditions. The mixture was then centrifugation, rinsed thrice with deionized water, and dried in a hot air oven at 150 °C for one hour. Afterwards, the specimens were served as the SHA and sintered for one hour at 700 °C.

Fabrication of the HSAC bioscaffold sponges: A modified approach published by Han *et al*. (2021) was used to produce HLR leaves extract by percolation. ALG was homogeneously dissolved in 100 mL of DW using an ultrasonication process that lasted 30 min. HLR was subsequently added to the mixture to create a mixed solution with two distinct concentrations (3 % and 7 %). The ALG/HLR solution was placed into the a 96-well plate and chilled at 36 °C night before being lyophilized in a freeze-dryer at 50 °C under vacuum for 2 days. The ALG/HLR was then soaked in CMC/SHA and lyophilized to produce HSAC bioscaffold sponges. Following the procedures, bioscaffold sponges with two distinct HLR percentages were labeled HSAC-I and HSAC-II. The ALG/CMC/SHA bioscaffold sponges were made in the same manner as described above. Schematic representing the concept of using substituted hydroxyapatite, biopolymers, and herbal such as HSAC bioscaffold sponge for burn wound healing applications (Fig. 1).

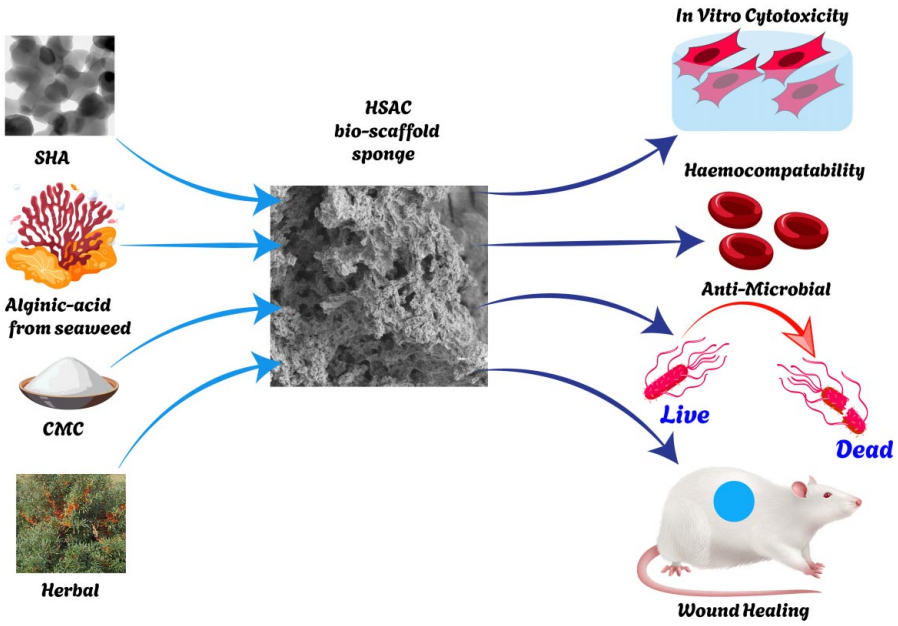

Fig. 1. Schematic representing the concept of using substituted hydroxyapatite, biopolymers, and herbal such as HSAC bioscaffold sponge for burn wound healing applications.

Physicochemical characterization: Scanning electron microscope (S-4800, Japan) and high-resolution transmission electron microscopy (JEOL, Japan) were used to examine the morphology of the produced samples. FTIR spectra (Nicolet iN10) were utilized to describe the materials in the 500-4000 cm^{-1} range. The water vapor transmission rate (WVTR) was determined using the American Society for Testing and Materials (E-96-00) method.

Antibacterial activity: Bacterial cells (*S. aureus* and *E. coli*) were grown overnight at 37 °C with 300 rpm in Mueller-Hinton broth (MHB). Following that, 1 mL of bacterial culture containing 1X 107 CFU/mL was applied to the top of a 96-well sized bioscaffold and incubated for one day at 37 °C. Following a series of dilutions and shaking for ten min, the aliquots of culture media and microbial attached bioscaffold were placed into a sterile tube containing 10 mL Phosphate buffer. The mixture was then distributed on Luria-Bertani agar plates. After one day of incubation in an anaerobic room, the number of colonies was measured using a comet assay.

Biocompatibility assay: The CCK-8 test was used to measure Human Umbilical Vein Endothelial Cells (HUVEC) cell multiplication. HUVECs were enumerated using a hemato-cytometer underneath a microscopy, and a ratio of 5×10^4 cells/mL was created in full medium. HUVECs were then sown in a 96-well microplate. The culture media was replenished with various amounts of specimens after one day of cell adhesion. Cell viability was determined using the CCK-8 test after 1, 3, and 7 days. The supernatants were removed and measured at 450 nm with a microplate (n = 3).

***In vivo* study:** All *in vivo* research were authorized by pharmaceutical department, The First Hospital of Tsinghua University Animal Care and Use Committee in accordance with the guidelines (JN.NO20221030RO300818). All rats were handled adequately during the study. To acclimate, all mature SD rats were given food for 48h. The healing and recovery therapeutic efficacy of bioscaffold sponge were tested using a Sprague-Dawley (SD) rat back burn models. After anesthesia with pentobarbital, the ventral fur of the SD rat was trimmed and washed with ethanol. Scorching thermal management equipment was used to generate scald wounds in the dorsal skin of each rat. Following that, positive control (MEBO), HSAC-1 and HSAC-2 were administered to the burns. Burns cured with no substances under identical conditions acted as the control. Pictures of burn (Digital camera (Meizu, China) regions were obtained after three, seven, and fourteen days and the burn area at each timestamp was calculated with Image J application (n = 5). The specimens were then coated with hematoxylin and eosin (H&E) and examined under a microscopy.

Statistical Analyses: The studies were conducted in triplicate and the resulting data were presented as the mean value along with the corresponding standard deviation (SD). The data was subjected to statistical analysis utilizing the one-way ANOVA.

RESULTS

Characterization of hydroxyapatite: X-Ray Diffraction (XRD), High-Resolution Transmission Electron Microscopy (HRTEM) and Energy Dispersive X-Ray Analysis (EDAX) were used to characterize the SHA, with the findings presented in Figure 2. The XRD analysis of SHA nanocrystals display prominent diffraction peaks at 34°, 32°, and 26°, which match closely to the covering diffraction of pure hydroxyapatite and the crystalline plane characteristic peaks (Fig. 2A) (Ahmed *et al*., 2022). HRTEM pictures reveal that distributed SHA nanocrystals exhibit a variety of

architectures, typically in the shape of spherical. In the meantime, SHA nanocrystals might develop uneven clusters (Fig. 2B). SHA crystals and clusters were observed in 100 nm. Figure 2C depicts the EDAX spectrum revealing the fundamental components of the SHA, which demonstrates the existence of Ca, Cu, Zn, C, O, and P in the corresponding SHA particle.

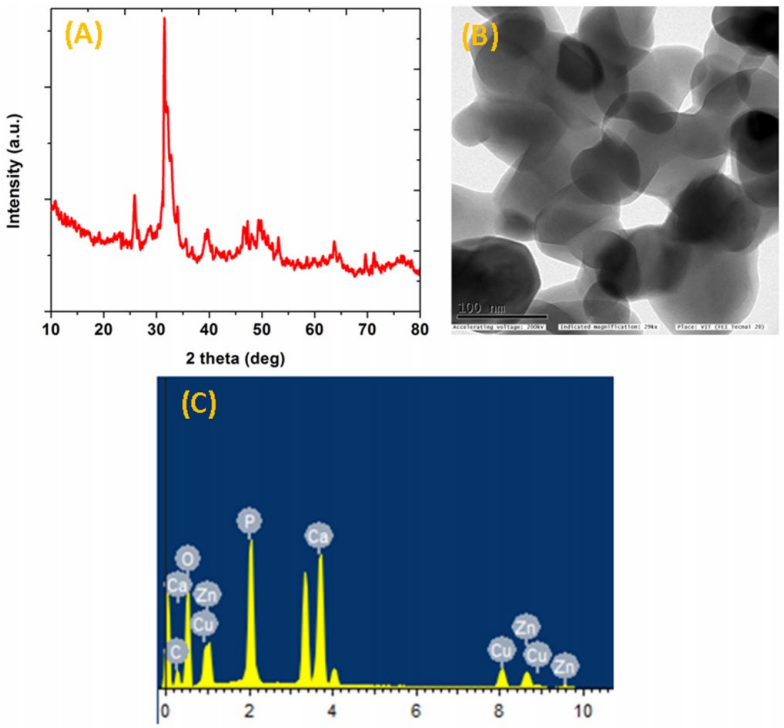

Fig. 2. the XRD pattern of SHA (A), the TEM image of SHA (B) and EDAX spectrum of SHA (C).

Characterization of composite: Figure 3 shows the FTIR spectra of ALG, CMC, HLR, SHA, HSAC-1 and HSAC-2 bioscaffold samples. The significant peaks in the ALG sample at 1418 cm^{-1} and 1589 cm^{-1} were ascribed to a symmetric and symmetric stretch vibration of COOH groups, respectively (Bajas *et al*., 2021). A typical CMC spectrum is noted, with an aggressive peak between 1202 and 956 cm^{-1} corresponding to the -C-O, C-CH stretching and bending of the glycoside ring, and -CO stretching, as well as a peak at 1410 cm^{-1} respective to the stretching mode of the polymer's free carboxylate groups (Wongvitvichot *et al*., 2021). HLR exhibits OH and carbonyl group absorption bands at 3381 to 3005 cm^{-1}, 1722 cm-1 and 1679 cm^{-1}, 1527 cm^{-1} (Lyu *et al*., 2021). These peaks demonstrated that the leaf extract contained phenolics and other flavonoids. The peaks between 1097 cm^{-1} and 1034 cm^{-1} revealed the existence of PO43- in SHA (Siswanto *et al*., 2020). The bioscaffold sponge band has all of the ALG/CMC/SHA and HLR characteristic peaks, indicating that HLR was integrated into the bioscaffold sponges. All of the detected peaks indicate that the biocomposites are a combination of ALG/CMC/SHA and HLR compounds that do not create new interfaces interactions.

Microscopically examining and evaluating the morphology of HSAC-1 and HSAC-2 bioscaffolds sponge were done using the SEM image. All prepared bioscaffold sponges showed a strongly linked, porous architecture and an uneven structure, which is advantageous for allowing sufficient space for exudates and blood absorption and so promoting faster wound healing (Fig. 4A) (Mahmoud & Salama, 2016). The pores of HSAC-2 are smaller and more equally distributed. The addition of HLR reduced the pore diameter of HSAC bioscaffold sponges from 130±15 to 85±10 µm, according to quantitative data on pore diameter (Fig. 4B). In the conditions of introducing HLR proportions of 3 % and 7 %, a highest porosity of 89 ± 5.7 % was attained at HSAC-1, and the values of HSAC-1 was 50 ± 5 % (Fig. 4C). The increased porosity helps to keep the wound wet while also promoting cell growth and wound repair (Hu *et al*., 2018).

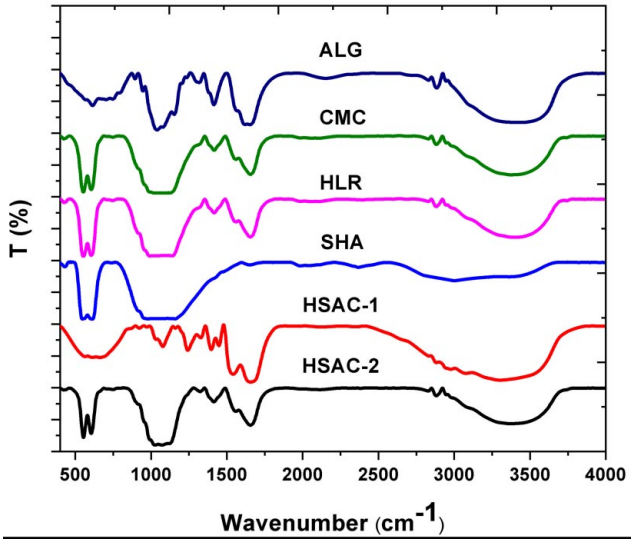

Fig. 3. FTIR spectra of ALG, CMC, HLR, SHA, HSAC-1 and HSAC-2.

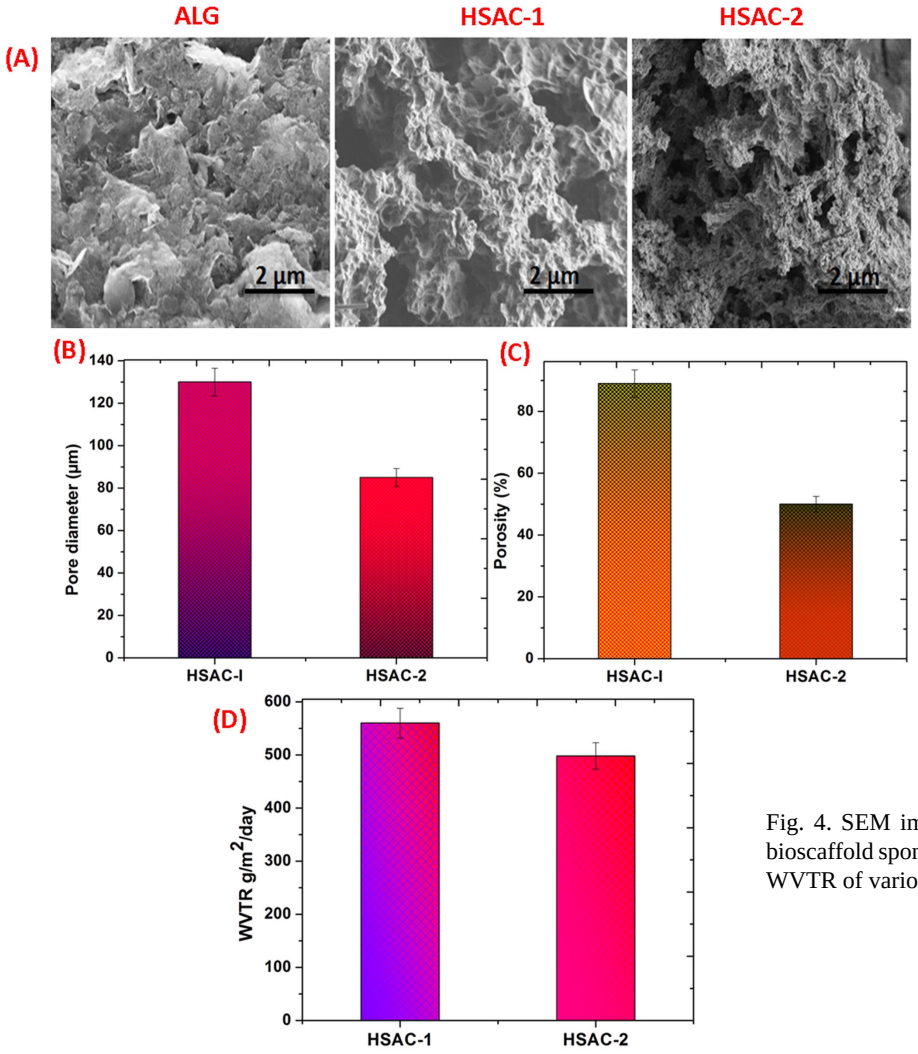

Fig. 4. SEM images of ALG, HSAC-1 and HSAC-2 bioscaffold sponges (A), Pore size (B), porosity (C) and WVTR of various bioscaffold samples (D).

Water vapor transmission rate: The water vapor transmission rate (WVTR) of HSAC-1 was above 500 g, as shown in Figure 4D, but HSAC-2 values were a little lower. Given that the thick architecture was not beneficial to WVTR at the same water content, this result may be related to pore permeability and size. In general, the needed WVTR of wounded skin ranges from 279 to 5318, depending on the extent of the skin disorders, and the WVTR of HSAC bioscaffold sponges may meet the porosity criteria of wound dressings. The porous nature of sponges allows for oxygen delivery, which aids in wound preventing infection, and airflow on the incision site can increase the aggregation of clotting factors, platelets, and fibrinogen to accomplish clotting (Varalakshmi *et al*., 2015).

Antibacterial activity:In this study, two common microorganisms (*S. aureus* and *E. coli*) were used to assess the bioscaffold sponge's antibacterial effectiveness. The results demonstrated that both HSAC-1 and HSAC-2 have outstanding bactericidal characteristics; although, there is no significant difference in bactericidal efficiency between HSAC-1 and HSAC-2. HLR and SHA combined antibacterial activity in bioscaffold sponge's accounts for their exceptional innate antibacterial capability (Figs. 5 A and B). As a result, bioscaffold sponges are appealing for use in wound care.

Hemolysis test: A prepared wound dressing's compatibility with blood cells is believed to be essential for wound healing. The hemolysis tests employed the two-percentage rabbit hemocyte solution. Figure 5C depicts the results, which reveal that significant hemolysis was observed in distilled water but not in saline solution. When comparing HSAC-1 and HSAC-2, little hemolysis was seen, with HSAC-2 displaying stronger suitability than HSAC-1 with a haemolytic rate of 4.37 %.

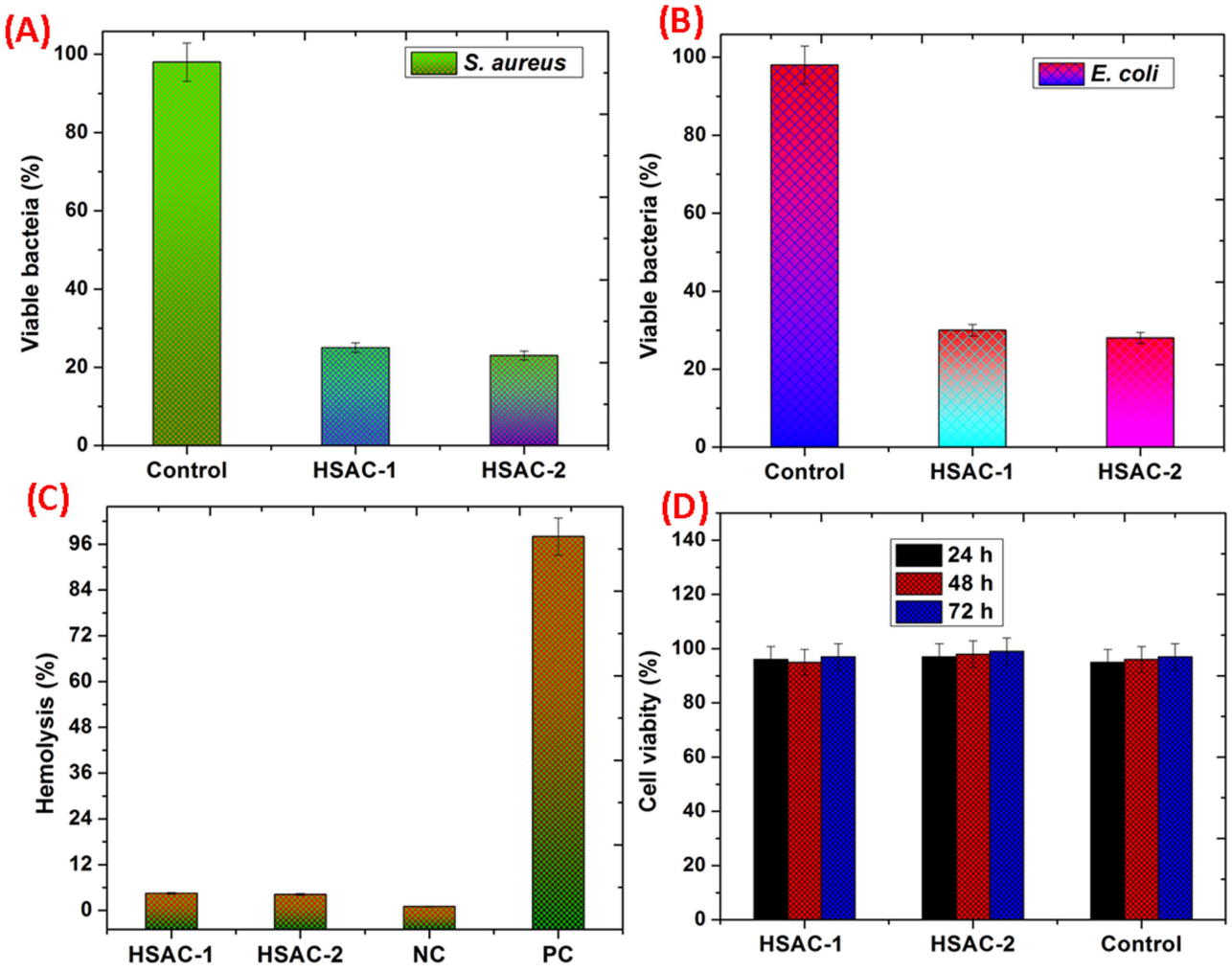

Fig. 5. Survival rate of *S. aureus* (A), *E. coli* after contact with different samples for 24 h (B), the results of hemolysis tests of samples (C), the results of cytotoxicity tests (D).

Cytocompatibility assay: The findings of the cell survival test demonstrated bioscaffold sponge's excellent biocompatibility, as shown in Figure 5D. Both HSAC-1 and HSAC-2 had considerably greater cell viability than the control after 24 hours. HSAC-2 had considerably greater cell viability than HSAC-1 and the control group after 48 hours. Conversely, after 72 hours, HSAC-2 has much higher cell viability than the control group whereas HSAC-1 has significantly lower vitality. As a result of its significant favorable influence on cell development, HSAC-2 hydrogel has proved appropriate for cell growth and good compatibility.

***In vivo* wound healing study:** On days 3, 7, and 21 following the injury, there was evidence of wound contraction (Fig. 6). The results showed that HSAC-2 bioscaffold were efficient in wound repair as early as the 3rd day. In contrast to the control group, the HSAC-1 and HSAC-2 groups had significant wound-healing activity. Interestingly, significant healing was observed in the HSAC-2 group on day 14.

Figure 6B depicts the evolution of burn tissue repair rates in Wister rats over time. The HSAC-1 and HSAC-2 groups healed considerably quicker than the control group on day 14. Additionally, compared to the positive control group, the HSAC-2 bioscaffold showed a much greater healing rate.

Figure 6C shows photomicrographs of the specimens for histological investigation that were collected from all samples on the 3rd, 7th, and 14th days following treatment. HSAC bioscaffold groups showed complete healing on day 14th. On the 14th day, the HSAC-2 group demonstrated full recovery. The positive control and HSAC-1 groups, on the other hand, showed moderate inflammation and significant vasculature. Furthermore, in the HSAC-2 group, full epidermal rejuvenation was found, indicating that the formulation enhances wound healing.

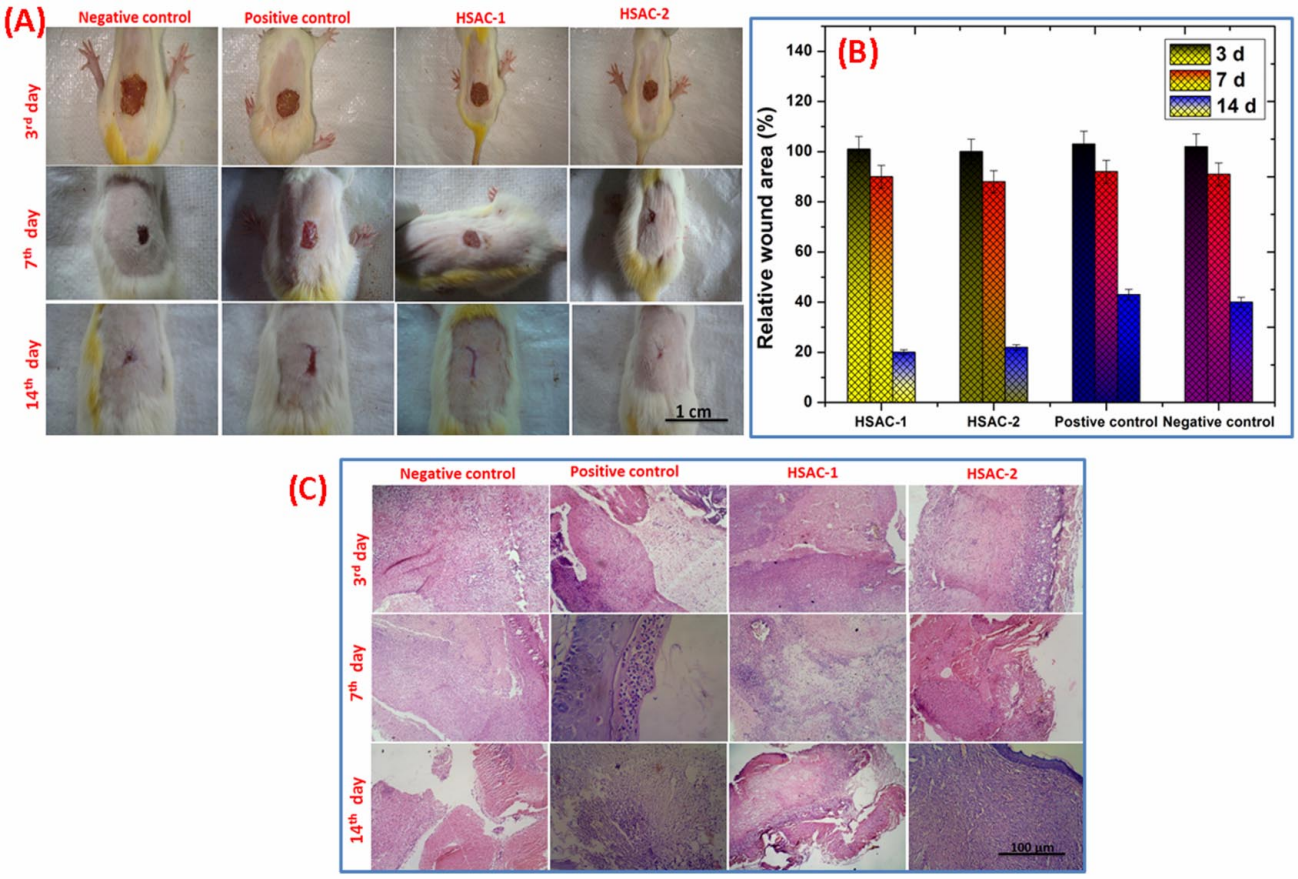

Fig. 6. Digital photos of burns that were covered with negative control (physiological saline solution), positive control MEBO, HSAC-1 and HSAC-2 within 14 days (A), % of burns size over time (B) and histopathological slides of treated animals (C).

DISCUSSION

The present study successfully synthesized a novel hydroxyapatite (HA)-based bioscaffold incorporating *Hippophae rhamnoides* L (HLR) extract. This bioscaffold demonstrated promising potential for wound healing applications. The synthesized HA nanocrystals exhibited characteristic diffraction peaks in XRD analysis, confirming their crystalline structure and purity. HRTEM images revealed a spherical morphology with uneven clustering, suggesting a potential for enhanced surface area and interaction with biological components. EDAX analysis confirmed the presence of essential elements (Ca, Cu, Zn, C, O, and P) within the HA particles. FTIR analysis indicated the successful incorporation of HLR into the HA/ALG/CMC bioscaffold. The presence of characteristic peaks for HLR, HA, ALG, and CMC confirmed the formation of a composite material without significant interactions between components. SEM analysis revealed a porous structure, essential for exudate absorption and cell migration. The addition of HLR reduced pore diameter and increased porosity, enhancing the scaffold's suitability for wound healing. The WVTR of the bioscaffolds was within the desired range for wound dressings, ensuring adequate moisture retention and oxygen exchange. The porous structure of the scaffolds contributed to this favorable property. The bioscaffolds demonstrated excellent antibacterial activity against both *S. aureus* and *E. coli*. The combination of HLR and HA likely contributed to the enhanced antimicrobial properties. The bioscaffolds exhibited low hemolysis and high cytocompatibility, indicating their biocompatibility and potential for minimizing adverse reactions during wound healing. The *in vivo* study demonstrated the efficacy of the bioscaffolds in wound healing. The HSAC-2 formulation, containing a higher concentration of HLR, exhibited superior wound healing compared to the control and HSAC-1 groups. Histological analysis confirmed the bioscaffold's ability to promote tissue regeneration and reduce inflammation.

CONCLUSION

In conclusion, microwave method was used to synthesize substituted hydroxyapatite nanoparticle. Furthermore, using lyophilization procedures, HSAC multifunctional biocomposite sponges were effectively made by incorporating *Hippophae rhamnoides* L (HLR) into substituted hydroxyapatite (SHA)/alginate (ALG)/ carboxymethyl cellulose (CMC). The HLR-containing synthesized SHA/ALG/CMC bioscaffold formulation induces an amazing level of wound-healing activity. It demonstrated considerable wound-healing activity and may be considered as an innovative pharmacological therapy in the treatment of burn wounds. The current work may give a unique technique for wound healing employing HLR bioscaffolds.

XU, M. y ZHU, X. La esponja de bioandamio con *Hippophae rhamnoides* L acelera la reparación de heridas por quemaduras: estudios *in vitro* e *in vivo*. *Int. J. Morphol., 43(2)*:351-359, 2025.

RESUMEN: Varios materiales para apósitos de heridas tienen defectos funcionales y estructurales que les impiden facilitar la cicatrización de heridas. La aceleración de la coagulación sanguínea, prevención de la infección bacteriana e iniciar el proceso de regeneración en heridas de espesor total son todos resultados posibles del diseño de apósitos multifuncionales para heridas. En este trabajo, se combinó *Hippophae rhamnoides* L (HRL), una hierba tradicional china, con hidroxiapatita sustituida (SHA)/alginato (ALG)/ carboximetilcelulosa (CMC) (HSAC) mediante técnicas de secado por congelación, atracción electrostática y reticulación ecológica para fabricar esponjas de bioandamio multifuncionales. La proliferación celular de las muestras de HSAC mejoró considerablemente en comparación con el control para diferentes tiempos de cultivo celular. Mientras que el estudio *in vivo* se llevó a cabo utilizando un modelo de herida por escisión, las investigaciones *in vitro* se llevaron a cabo utilizando ensayos de toxicidad y cicatrización de heridas. La histología se realizó en tejidos extraídos de la región de la herida. Observamos el proceso de cicatrización de la herida durante uno, tres y catorce días. La formulación de esponja de bioandamio que contenía HRL tuvo un mejor desempeño que el grupo control cuando se evaluó la construcción de la herida. El análisis histológico mostró que la formulación de HRL indujo la actividad regenerativa de la piel. El experimento de cicatrización de heridas utilizando células HUVEC reveló una proliferación celular significativa cuando se utilizaron esponjas de bioandamio con HRL. Finalmente, tanto *ex vivo* como *in vivo*, nuestro material de prueba, las esponjas de bioandamio HSAC, aceleraron significativamente la cicatrización de heridas.

PALABRAS CLAVE: Bioandamio; Actividad antibacteriana; Heridas por quemaduras; Hierbas; Cicatrización de heridas.

REFERENCES

Ahmed, H. Y.; Safwat, N.; Shehata, R.; Althubaiti, E. H.; Kareem, S.; Atef, A.; Qari, S. H.; Aljahani, A. H.; Al-Meshal, A. S.; Youssef, M.; *et al.* Synthesis of natural nano-hydroxyapatite from snail shells and its biological activity: antimicrobial, antibiofilm, and biocompatibility. *Membranes (Basel), 12(4)*:408, 2022.

Bajas, D.; Vlase, G.; Mateescu, M.; Grad, O. A.; Bunoiu, M.; Vlase, T. & Avram, C. Formulation and characterization of alginate-based membranes for the potential transdermal delivery of methotrexate. *Polymers (Basel), 13(1)*:161, 2021.

Chang, G.; Dang, Q.; Liu, C.; Wang, X.; Song, H.; Gao, H.; Sun, H.; Zhang, B. & Cha, D. Carboxymethyl chitosan and carboxymethyl cellulose based self-healing hydrogel for accelerating diabetic wound healing. *Carbohydr. Polym., 292*:119687, 2022.

Chen, A.; Feng, X.; Dorjsuren, B.; Chimedtseren, C.; Damda, T. A. & Zhang, C. Traditional food modern food and nutritional value of Sea buckthorn (*Hippophae rhamnoides* L.): a review. *J. Future Foods, 3(3)*:191-205, 2023.

Hegde, V.; Uthappa, U. T.; Altalhi, T.; Jung, H. Y.; Han, S. S. & Kurkuri, M. D. Alginate based polymeric systems for drug delivery antibacterial/ microbial and wound dressing applications. *Mater. Today Commun., 33*:104813, 2022.

Han, Y.; Yuan, C.; Zhou, X.; Han, Y.; He, Y.; Ouyang, J.; Zhou, W.; Wang, Z.; Wang, H. & Li, G. Anti-inflammatory activity of three triterpene from *Hippophae rhamnoides* L. in lipopolysaccharide-stimulated RAW264.7 *Cells. Int. J. Mol. Sci., 22(21)*:12009, 2021.

Hu, S.; Bi, S.; Yan, D.; Zhou, Z.; Sun, G.; Cheng, X. & Chen, X. Preparation of composite hydroxybutyl chitosan sponge and its role in promoting wound healing. *Carbohydr. Polym., 184*:154-63, 2018.

Jafari, M.; Baniasadi, H.; Rezvanpour, A. & Lotfi, M. Fabrication and characterisation of a wound dressing composed of polyvinyl alcohol and quince seed mucilage. *J. Wound Care, (Sup9a)*:XIIIi-XIIIx, 2021.

Kamoun, E. A.; Kenawy, E. R. & Chen, X. A review on polymeric hydrogel membrane for wound dressing applications PVA-based hydrogel dressings. *J. Adv. Res., 8(3)*:217-33, 2017.

Kumar, R. & Mohanty, S. Hydroxyapatite a versatile bioceramic for tissue engineering application. *J. Inorg. Organomet. Polym. Mater.*, 1-18, 2023.

Lyu, X.; Wang, X.; Wang, Q.; Ma, X.; Chen, S. & Xiao, J. Encapsulation of sea buckthorn (*Hippophae rhamnoides* L.) leaf extract via an electrohydrodynamic method. *Food Chem., 365*:130481, 2021.

Ma, Q. G.; He, N. X.; Huang, H. L.; Fu, X. M.; Zhang, Z. L.; Shu, J. C.; Wang, Q. Y.; Chen, J.; Wu, G.; Zhu, M. N.; et al. *Hippophae rhamnoides* L.: a comprehensive review on the botany, traditional uses, phytonutrients, health benefits, quality markers, and applications. *J. Agric. Food Chem., 71(12)*:4769-88, 2023.

Mahmoud, A. A. & Salama, A. H. Norfloxacin-loaded collagen/chitosan scaffolds for skin reconstruction: Preparation, evaluation and *in-vivo* wound healing assessment. *Eur. J. Pharm. Sci., 83*:155-65, 2016.

Pundir, S.; Garg, P.; Dviwedi, A.; Ali, A.; Kapoor, V. K.; Kapoor, D.; Kulshrestha, S.; Lal, U. R. & Negi, P. Ethnomedicinal uses, phytochemistry and dermatological effects of *Hippophae rhamnoides* L.: A review. *J. Ethnopharmacol., 266*:113434, 2021.

Raus, R. A.; Nawawi, W. M. & Nasaruddin, R. R. Alginate and alginate composites for biomedical applications. *Asian J. Pharm. Sci., 16(3)*:280-306, 2021.

Saavedra, P. A. E.; De Oliveira Leal, J. V.; Areda, C. A. & Galato, D. The costs of burn victim hospital care around the world a systematic review. *Iran. J. Public Health., 50(5)*:866-78, 2021.

Sahoo, D. R. & Biswal, T. Alginate and its application to tissue engineering. *SN Appl. Sci., 3*:30, 2021.

Siswanto, S.; Hikmawati, D.; Kulsum, U.; Rudyardjo, D. I.; Apsari, R. & Aminatun, A. Biocompatibility and osteoconductivity of scaffold porous composite collagen–hydroxyapatite based coral for bone regeneration. *Open Chem., 18(1)*:584-90, 2020.

Varalakshmi, V.; Suganiya, S. A. & Mala, R. Fabrication and characterization of hybrid sponge for healing of infectious burn wound. *Recent Pat. Nanotechnol., 9(3)*:212-21, 2015.

Widiyanti, P. & Priskawati, Y. C. A. Synthesis and characterization of hydrogel-based hyaluronic acid-chitosan-allium sativum extract for intraperitoneal antiadhesion application. *Int. J. Biomater., 2023*:5172391, 2023.

Wang, Y. & Shi, D. In vitro and in vivo evaluations of nanofibrous nanocomposite based on carboxymethyl cellulose/polycaprolactone/cobalt-doped hydroxyapatite as the wound dressing materials. *Arab. J. Chem., 15(11)*:104270, 2022.

Wongvitvichot, W.; Pithakratanayothin, S.; Wongkasemjit, S. & Chaisuwan, T. Fast and practical synthesis of carboxymethyl cellulose from office paper waste by ultrasonic-assisted technique at ambient temperature. *Polym. Degrad. Stab., 184*:109473, 2021.

Yu, Y.; Lin, C.; Wu, M. & Tao, B. Fabrication of copper ions-substituted hydroxyapatite coating on titanium substrates for antibacterial and osteogenic applications. *Mater. Lett., 307*:131072, 2022.

Zhang, H.; Chen, C.; Zhang, H.; Chen, G.; Wang, Y. & Zhao, Y. Janus medical sponge dressings with anisotropic wettability for wound healing. *Appl. Mater. Today, 23*:101068, 2021.

Corresponding author:
Ming Xu
Pharmaceutical Department
The First Hospital of Tsinghua University
Beijing 100016
CHINA

E-mail: xuming1370117@sina.com

Xingyu Zhu
University of Technology and Science Beijing
School of Mathematics and Physics
U202242316
30 Xueyuan Road
Haidian District
Beijing 100083
CHINA

E-mail: 18811022631@163.com